

# Cloaking using anisotropic multilayer circular cylinder

Cite as: AIP Advances 10, 095312 (2020); <https://doi.org/10.1063/5.0012769>

Submitted: 05 May 2020 . Accepted: 17 August 2020 . Published Online: 08 September 2020

Sidra Batool , Mehwish Nisar , Fabio Mangini, and Fabrizio Frezza 

## COLLECTIONS

Paper published as part of the special topic on [Chemical Physics](#), [Energy, Fluids and Plasmas](#), [Materials Science](#) and [Mathematical Physics](#)



View Online



Export Citation




CrossMark



**NEW!**

Sign up for topic alerts  
New articles delivered to your inbox



# Cloaking using anisotropic multilayer circular cylinder

Cite as: AIP Advances 10, 095312 (2020); doi: 10.1063/5.0012769

Submitted: 5 May 2020 • Accepted: 17 August 2020 •

Published Online: 8 September 2020



View Online



Export Citation



CrossMark

Sidra Batool,<sup>1,a)</sup>  Mehwish Nisar,<sup>1</sup>  Fabio Mangini,<sup>2</sup> and Fabrizio Frezza<sup>1</sup> 

## AFFILIATIONS

<sup>1</sup>Department of Information Engineering, Electronics and Telecommunications, “La Sapienza” University of Rome, Via Eudossiana 18, 00184 Rome, Italy

<sup>2</sup>Department of Information Engineering, University of Brescia, Via Branze 38, 25123 Brescia, Italy

<sup>a)</sup> Author to whom correspondence should be addressed: [sidra.batool@uniroma1.it](mailto:sidra.batool@uniroma1.it)

## ABSTRACT

In this article, we study a homogenization model for cloaking applications. In the given model, we consider an isotropic inner layer, which is coated with a multilayer anisotropic circular cylinder. We describe the electrostatic response of a polarly radially anisotropic (PRA) multilayer circular cylinder. It consists of different components of permittivity in radial and tangential directions for each layer. We have shown the mathematical derivation of the polarizability and effective permittivity of a PRA multilayer circular cylinder. Moreover, we demonstrate the cloaking behavior using a PRA multilayer circular cylinder. Meanwhile, we test our formation with advanced computational approaches. During our numerical test, we have investigated the numerical results of the polarizability of a PRA multilayer circular cylinder. We employ an inner cloak surrounded by a multilayer anisotropic circular cylinder. However, for an ideal cloak, the contrast between the permittivity parameters approaches infinity.

© 2020 Author(s). All article content, except where otherwise noted, is licensed under a Creative Commons Attribution (CC BY) license (<http://creativecommons.org/licenses/by/4.0/>). <https://doi.org/10.1063/5.0012769>

## I. INTRODUCTION

There has been growing interest in the scientific community and the general public in optical cloaking in recent years. Basically, the object has been surrounded by a cloak in such a way that the whole structure becomes invisible.<sup>1–4</sup> Cloak material exhibits special and exotic optical properties that are favorable for making any object invisible irrespective of its size and shape. The first and one of the most powerful approaches toward designing and implementation of cloaking devices has been called transformation optics.<sup>5–8</sup> It determines the conditions under which incident light can be controlled to move around the object without distortion. The other popular technique is plasmonic cloaking,<sup>9,10</sup> which has been developed to study scattering from plasmonic and metamaterial coatings.

Many different techniques that can minimize distortion in an incident electric field have been considered within full-wave scattering theory.<sup>11–14</sup> For this to happen, different analytical conditions have been derived that dictate the properties of multilayer coating. One of the popular ways is to employ radially anisotropic (RA) permittivity rather than isotropic permittivity.<sup>15–17</sup> A general algorithm

that applies to the cloak has been proposed, which employs an inhomogeneous and anisotropic cloak which is discretized into multiple homogeneous anisotropic layers.<sup>18–21</sup>

Other techniques that are based on Mie scattering theory have been worked out for multilayer anisotropic spherical shells.<sup>22</sup> Cloaking under the quasi-static limit using RA coatings has also been suggested.<sup>22,23</sup> Gao *et al.*<sup>18</sup> proposed the cancellation of the dipole moments of radially anisotropic spheres using suitable RA coatings. Kettunen *et al.*<sup>23</sup> have also proposed a model that studies the cloaking of small objects.

Kettunen *et al.*<sup>23</sup> employ spherical and cylindrical objects covered by a single radially anisotropic layer. The particle can be invisible if there exists a certain relationship between the tangential and radial parts of the RA shell. When a tangential component of the shell approaches infinity and the radial component approaches zero, the cloak has to cancel the excitation field in its interior.

In this paper, we generalize the work of Kettunen *et al.*<sup>23</sup> that discusses cylindrical geometry. A dielectric cylinder is surrounded by many anisotropic layers, and each layer has different radially anisotropic permittivities. Based on quasi-static approximation,

potentials have been derived as analytic solutions to Laplace’s equation. We described the polarizability and effective permittivity for the whole structure. It is placed in free space with a vacuum permittivity  $\epsilon_0$ , and the radial and tangential permittivity components in each layer of the structure are assumed to be positive.

## II. FORMATION

### A. Effective permittivity and polarizability of a PRA multilayer cylinder

Let us consider a circular stratified cylinder object with radial anisotropy. In other words, we intend to see the desired cloaking effect by using the transverse electric excitation response of a cylinder. Because of the axial-symmetry of the problem and the direction of the electric excitation, the axial electric part of the field is not excited, and the axial permittivity component  $\epsilon_z$  may have an arbitrary value. For this reason, the axial component is omitted in our analysis. The inspection of the multilayer cylinder with alternating relative permittivities  $\bar{\epsilon}_1$  and  $\bar{\epsilon}_2$ , immersed in a vacuum, is presented in Fig. 1.

The radius of the outer circular cylinder is fixed ( $a_1$ ), and the other internal radii can be written as<sup>24–26</sup>

$$a_k = \frac{N - (k - 1)}{N} a_1. \tag{1}$$

We consider the case of an equidistant layer cylinder. The number of layers ( $N$ ) is fully arbitrary. In cylindrical coordinates, the dielectric permittivity may be given as

$$\epsilon_P = \epsilon_0 (\epsilon_\rho \mathbf{u}_\rho \mathbf{u}_\rho + \epsilon_\phi \mathbf{u}_\phi \mathbf{u}_\phi). \tag{2}$$

It can be noted that the solution to the problem is independent of the direction of the application of the electric field and the multilayer circular cylinder core is isotropic and all outer  $N$  layers are anisotropic in a certain Cartesian frame of reference. Let us assume that the whole structure is excited by a uniform  $x$  polarized electric

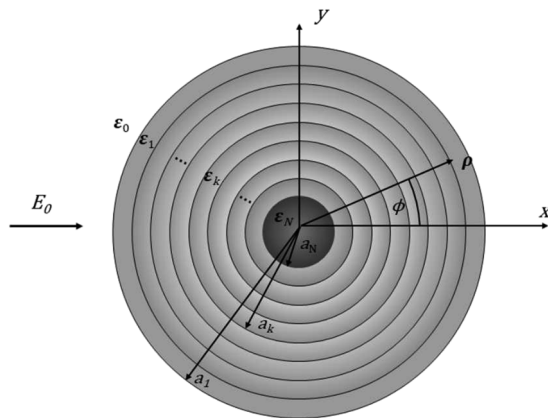


FIG. 1. Multilayer circular cylindrical structure. The inner isotropic core is coated with multilayer anisotropic material.

field,<sup>24,27</sup>

$$\mathbf{E}_0 = \mathbf{u}_x E_0 = \mathbf{u}_x \frac{U_0}{a_k}. \tag{3}$$

Here,  $U_0$  indicates the difference in the potential across the cylinder radius  $a_k$ . The solution of the Laplace equation in the  $k$ th isotropic region is<sup>27–29</sup>

$$\Phi_k = -B_k \rho \cos \phi + C_k \rho^{-1} \cos \phi, \tag{4}$$

and that for the  $k$ th anisotropic subregion is

$$\Phi_k = -B_k \rho^{\gamma_k} \cos \phi + C_k \rho^{-\gamma_k} \cos \phi, \tag{5}$$

where

$$\gamma_k = \sqrt{\frac{\epsilon_\phi}{\epsilon_\rho}}. \tag{6}$$

Let us consider a case where the structure is composed of an alternating sequence (isotropic to anisotropic) of layers. Then, Eq. (4) represents the potential of the  $N$  layer structure for the  $k$ th isotropic subregion, and the consecutive anisotropic layer is

$$\Phi_{k+1} = -B_{k+1} \rho^{\gamma_{k+1}} \cos \phi + C_{k+1} \rho^{-\gamma_{k+1}} \cos \phi. \tag{7}$$

By applying boundary conditions, we obtain

$$\Phi_k = \Phi_{k+1} \quad \rho = a_{k+1}, \tag{8}$$

$$\epsilon_{\rho k} \frac{\partial \Phi_k}{\partial \rho} = \epsilon_{\rho k+1} \frac{\partial \Phi_{k+1}}{\partial \rho} \quad \rho = a_{k+1}. \tag{9}$$

The resulting equations can be written in a matrix form as<sup>30–32</sup>

$$\begin{pmatrix} B_k \\ C_k \end{pmatrix} = [M_k] \begin{pmatrix} B_{k+1} \\ C_{k+1} \end{pmatrix}, \tag{10}$$

where

$$[M_k] = \frac{1}{2\epsilon_k} \begin{pmatrix} M_{k11} & M_{k12} \\ M_{k21} & M_{k22} \end{pmatrix}, \tag{11}$$

and

$$\begin{pmatrix} B_k \\ C_k \end{pmatrix} = \frac{1}{2\epsilon_k} \begin{pmatrix} M_{k11} & M_{k12} \\ M_{k21} & M_{k22} \end{pmatrix} \begin{pmatrix} B_{k+1} \\ C_{k+1} \end{pmatrix}, \tag{12}$$

where

$$\begin{aligned} M_{k11} &= (\gamma_{k+1} \epsilon_{k+1} + \epsilon_k) a_{k+1}^{\gamma_{k+1}-1} \\ M_{k12} &= (-\epsilon_k + \gamma_{k+1} \epsilon_{k+1}) a_{k+1}^{-\gamma_{k+1}-1} \\ M_{k21} &= (-\epsilon_k + \gamma_{k+1} \epsilon_{k+1}) a_{k+1}^{\gamma_{k+1}+1} \\ M_{k22} &= (\epsilon_k + \gamma_{k+1} \epsilon_{k+1}) a_{k+1}^{-\gamma_{k+1}+1} \end{aligned}$$

Similarly, the generalized propagation matrix for two adjacent anisotropic layers is

$$\begin{pmatrix} B_k \\ C_k \end{pmatrix} = \frac{1}{2\epsilon_k \gamma_k} \begin{pmatrix} P_{k11} & P_{k12} \\ P_{k21} & P_{k22} \end{pmatrix} \begin{pmatrix} B_{k+1} \\ C_{k+1} \end{pmatrix}, \tag{13}$$

where

$$\begin{aligned} P_{k11} &= (\gamma_{k+1}\epsilon_{k+1} + \gamma_k\epsilon_k)a_{k+1}^{\gamma_{k+1}-\gamma_k} \\ P_{k12} &= (\gamma_k\epsilon_k - \gamma_{k+1}\epsilon_{k+1})a_{k+1}^{-\gamma_{k+1}-\gamma_k} \\ P_{k21} &= (\gamma_k\epsilon_k - \gamma_{k+1}\epsilon_{k+1})a_{k+1}^{\gamma_{k+1}+\gamma_k} \\ P_{k22} &= (\gamma_k\epsilon_k + \gamma_{k+1}\epsilon_{k+1})a_{k+1}^{-\gamma_{k+1}+\gamma_k} \end{aligned}$$

In addition, the generalized propagation matrix for two adjacent anisotropic and isotropic layers is

$$\begin{pmatrix} B_k \\ C_k \end{pmatrix} = \frac{1}{2\epsilon_k\gamma_k} \begin{pmatrix} Q_{k11} & Q_{k12} \\ Q_{k21} & Q_{k22} \end{pmatrix} \begin{pmatrix} B_{k+1} \\ C_{k+1} \end{pmatrix}, \quad (14)$$

where

$$\begin{aligned} Q_{k11} &= (\gamma_k\epsilon_k + \epsilon_{k+1})a_{k+1}^{-\gamma_k+1} \\ Q_{k12} &= (\gamma_k\epsilon_k - \epsilon_{k+1})a_{k+1}^{-\gamma_k-1} \\ Q_{k21} &= (\gamma_k\epsilon_k - \epsilon_{k+1})a_{k+1}^{\gamma_k+1} \\ Q_{k22} &= (\gamma_k\epsilon_k + \epsilon_{k+1})a_{k+1}^{\gamma_k-1} \end{aligned}$$

When  $\gamma_k = \gamma_{k+1} = 1$ , all the above generalized expressions are reduced into an isotropic multilayer structure.<sup>24</sup>

### III. SPECIAL CASES

When we consider all layers, the following relation is obtained:

$$\begin{pmatrix} B_0 \\ C_0 \end{pmatrix} = [M] \times \prod_{i=0}^{N-2} [P_i] \times [Q] \begin{pmatrix} B_N \\ 0 \end{pmatrix}. \quad (15)$$

We note that there is no reflected field  $C_N$  in the core region, i.e.,  $C_N = 0$ . For the special case  $N = 1$ ,  $[P] = 1$ , and  $[Q] = 1$ , the generalized expression may be written as

$$\begin{pmatrix} B_0 \\ C_0 \end{pmatrix} = [M] \begin{pmatrix} B_1 \\ C_1 \end{pmatrix}, \quad (16)$$

where

$$[M] = \frac{1}{2\epsilon_0} \begin{pmatrix} M_{11} & M_{12} \\ M_{21} & M_{22} \end{pmatrix}. \quad (17)$$

The normalized polarizability can be obtained through the following relation:

$$\alpha_P = \frac{2\epsilon_0 A}{a_1^2} \frac{M_{21}}{M_{11}}. \quad (18)$$

Let us consider an example where we can determine the normalized polarizability of a dielectric cylinder in free space by considering the simplest case  $N = 1$ ; then, the simplified trivial solution may be written as

$$\alpha_P = 2 \frac{(\gamma_1\epsilon_1 - \epsilon_0)}{(\gamma_1\epsilon_1 + \epsilon_0)}. \quad (19)$$

Moreover, in the case of  $N = 2$ ,  $i = 0, 1, 2, 3, \dots$ , and  $[P_0] = 1$ , the simplified solution of Eq. (15) is

$$\begin{pmatrix} B_0 \\ C_0 \end{pmatrix} = [M] \times [Q] \begin{pmatrix} B_2 \\ C_2 \end{pmatrix}, \quad (20)$$

where

$$[S] = [M] \times [Q] = \frac{1}{2\epsilon_0} \begin{pmatrix} M_{11} & M_{12} \\ M_{21} & M_{22} \end{pmatrix} \times \frac{1}{2\gamma_k\epsilon_k} \begin{pmatrix} Q_{11} & Q_{12} \\ Q_{21} & Q_{22} \end{pmatrix}. \quad (21)$$

Hence, we have the polarizability of two concentric circular cylinders as

$$\alpha_P = \frac{2\epsilon_0 V}{a_1^2} \frac{S_{21}}{S_{11}}, \quad (22)$$

and

$$\begin{aligned} S_{11} &= \frac{1}{4\gamma_k\epsilon_k} (M_{11}Q_{11} + M_{12}Q_{21}) \\ S_{12} &= \frac{1}{4\gamma_k\epsilon_k} (M_{11}Q_{12} + M_{12}Q_{22}) \\ S_{21} &= \frac{1}{4\gamma_k\epsilon_k} (M_{21}Q_{11} + M_{22}Q_{21}) \\ S_{22} &= \frac{1}{4\gamma_k\epsilon_k} (M_{21}Q_{12} + M_{22}Q_{22}). \end{aligned}$$

This allows us to find the normalized polarizability,

$$\alpha_P = 2 \frac{(\gamma_1\epsilon_1 - \epsilon_0)(\gamma_1\epsilon_1 + \epsilon_2) + (\epsilon_0 + \gamma_1\epsilon_1)(\epsilon_2 - \gamma_1\epsilon_1) \left(\frac{a_2}{a_1}\right)^{2\gamma_1}}{(\epsilon_0 + \gamma_1\epsilon_1)(\gamma_1\epsilon_1 + \epsilon_2) + (\gamma_1\epsilon_1 - \epsilon_0)(\epsilon_2 - \gamma_1\epsilon_1) \left(\frac{a_2}{a_1}\right)^{2\gamma_1}}. \quad (23)$$

For a homogenized dielectric circular cylinder with a relative permittivity  $\epsilon_n$ , the polarizability is defined as

$$\alpha_P = 2 \frac{(\epsilon_n - 1)}{(\epsilon_n + 1)}. \quad (24)$$

Thus, the effective permittivity  $\epsilon_{eff,p}$  for the circular cylinder is

$$\alpha_P = 2 \frac{(\epsilon_{eff,p} - 1)}{(\epsilon_{eff,p} + 1)}, \quad (25)$$

with

$$\epsilon_{eff} = \epsilon_1\gamma_1 \frac{(\epsilon_1\gamma_1 + \epsilon_2) + (\epsilon_2 - \epsilon_1\gamma_1) \left(\frac{a_2}{a_1}\right)^{2\gamma_1}}{(\epsilon_1\gamma_1 + \epsilon_2) - (\epsilon_2 - \epsilon_1\gamma_1) \left(\frac{a_2}{a_1}\right)^{2\gamma_1}}. \quad (26)$$

For the case of  $N = 3$ , the simplified algebraic equation may be written as

$$\begin{pmatrix} B_0 \\ C_0 \end{pmatrix} = [M] \times [P_1] \times [Q] \begin{pmatrix} B_3 \\ C_3 \end{pmatrix}, \quad (27)$$

where

$$\begin{aligned} [M] \times [P_1] \times [Q] &= \frac{1}{2\epsilon_k} \begin{pmatrix} M_{11} & M_{12} \\ M_{21} & M_{22} \end{pmatrix} \times \frac{1}{2\gamma_k\epsilon_k} \begin{pmatrix} P_{11} & P_{12} \\ P_{21} & P_{22} \end{pmatrix} \\ &\times \frac{1}{2\gamma_k\epsilon_k} \begin{pmatrix} Q_{11} & Q_{12} \\ Q_{21} & Q_{22} \end{pmatrix}. \end{aligned} \quad (28)$$

Hence,

$$[R] = [M] \times [P_1] \times [Q], \tag{29}$$

and

$$\begin{aligned} R_{11} &= \frac{1}{8\gamma_1\gamma_2\epsilon_0\epsilon_1\epsilon_2} \{ (M_{11}P_{11} + M_{12}P_{21})Q_{11} + (M_{11}P_{12} + M_{12}P_{22})Q_{21} \} \\ R_{12} &= \frac{1}{8\gamma_1\gamma_2\epsilon_0\epsilon_1\epsilon_2} \{ (M_{11}P_{11} + M_{12}P_{21})Q_{12} + (M_{11}P_{12} + M_{12}P_{22})Q_{22} \} \\ R_{21} &= \frac{1}{8\gamma_1\gamma_2\epsilon_0\epsilon_1\epsilon_2} \{ (M_{21}P_{11} + M_{22}P_{21})Q_{11} + (M_{21}P_{12} + M_{22}P_{22})Q_{21} \} \\ R_{22} &= \frac{1}{8\gamma_1\gamma_2\epsilon_0\epsilon_1\epsilon_2} \{ (M_{21}P_{11} + M_{22}P_{21})Q_{12} + (M_{21}P_{12} + M_{22}P_{22})Q_{22} \} \end{aligned}$$

Further, the polarizability of three concentric circular cylinders is

$$\alpha_P = \frac{2\epsilon_0 V R_{21}}{a_1^2 R_{11}}. \tag{30}$$

Hence, the normalized polarizability is

$$\alpha_P = \frac{2(A_1A_2A_3 + A_4A_5A_3)\left(\frac{a_2}{a_1}\right)^{2\gamma_1} + (A_1A_5A_6 + A_4A_2A_6)\left(\frac{a_2}{a_1}\right)^{2\gamma_1}\left(\frac{a_3}{a_2}\right)^{2\gamma_2}}{(A_4A_2A_3 + A_1A_5A_3)\left(\frac{a_2}{a_1}\right)^{2\gamma_1} + (A_4A_5A_6 + A_1A_2A_6)\left(\frac{a_2}{a_1}\right)^{2\gamma_1}\left(\frac{a_3}{a_2}\right)^{2\gamma_2}}, \tag{31}$$

where

$$\begin{aligned} A_1 &= \gamma_1\epsilon_1 - \epsilon_0 \\ A_2 &= \gamma_2\epsilon_2 + \gamma_1\epsilon_1 \\ A_3 &= \gamma_2\epsilon_2 + \epsilon_3 \\ A_4 &= \epsilon_0 + \gamma_1\epsilon_1 \\ A_5 &= \gamma_2\epsilon_2 - \gamma_1\epsilon_1 \\ A_6 &= \epsilon_3 - \gamma_2\epsilon_2 \end{aligned}$$

The effective permittivity  $\epsilon_{eff}$  for the circular cylinder may be written as

$$\epsilon_{eff} = \frac{\gamma_1\epsilon_1(A_2A_3 + A_3A_5)\left(\frac{a_2}{a_1}\right)^{2\gamma_1} + (A_5A_6 + A_2A_6)\left(\frac{a_2}{a_1}\right)^{2\gamma_1}\left(\frac{a_3}{a_2}\right)^{2\gamma_2}}{(A_2A_3 - A_3A_5)\left(\frac{a_2}{a_1}\right)^{2\gamma_1} + (A_5A_6 - A_2A_6)\left(\frac{a_2}{a_1}\right)^{2\gamma_1}\left(\frac{a_3}{a_2}\right)^{2\gamma_2}}.$$

#### IV. MULTILAYER CYLINDER AS A CLOAK

If we want to obtain a design rule for an ideal PRA cloak, that should be  $\epsilon_{eff} = 1$ , which is already given in the literature. We are considering a simpler approximate approach if the radius of the inner cylinder vanishes. We are using these approximations in effective permittivities for every iteration,  $k \rightarrow N$ , and  $a_k \rightarrow 0$ . Consider the iterative case of  $N = 2$ ; then, the radius of the inner cylindrical core is zero, i.e.,  $a_2 = 0$ . Inserting this into (26),

$$\epsilon_{eff} \rightarrow \epsilon_1\gamma_1 = \sqrt{\epsilon_{\rho_1}\epsilon_{\varphi_1}}. \tag{32}$$

The structure can be invisible if

$$\epsilon_{\rho_1}\epsilon_{\varphi_1} = 1. \tag{33}$$

Similarly, for the case of  $N = 3$ , the radius of the inner core must be  $a_3 = 0$ . Using (32),

$$\epsilon_{eff, p} = \epsilon_2\gamma_2 = \sqrt{\epsilon_{\rho_2}\epsilon_{\varphi_2}}. \tag{34}$$

For cloaking, we have

$$\epsilon_{\rho_2}\epsilon_{\varphi_2} = 1. \tag{35}$$

Let us choose the permittivity components that satisfy the invisibility condition for the arbitrary  $k$ th number of the layer,

$$\epsilon_{\varphi_k} = \kappa_k, \quad \epsilon_{\rho_k} = \frac{1}{\kappa_k}, \tag{36}$$

where  $\kappa \in \mathbb{R}^+$  is an arbitrary number.

#### V. NUMERICAL RESULTS AND DISCUSSION

The numerical results of this article are divided into two parts. First, we describe the numerical results of the polarizability of the PRA multilayer circular cylinder as a function of  $N$  number of layers. Using (30), we obtain the generalized polarizability of the whole structure consisting of a dielectric cylinder covered by many anisotropic cylindrical layers. We have also derived the expressions for up to three layers in (19), (23), and (31) using our generalized expression. We plot the polarizability as a function of the number

of layers in our simulation. We have fixed the following parameters: radius of the inner core  $a_3 = 0.50$ , first shell  $a_2 = 0.75$ , and second shell  $a_1 = 1$ . The anisotropy ratio for the first shell is  $\gamma_1 = 5$ , and that for the second shell is  $\gamma_2 = 6$ . For all cases, the anisotropy ratio is  $\gamma = \{5, 6\}$  such that for two concentric PRA cylindrical layers,  $\gamma_1 = 5$  and  $\gamma_2 = 6$  and *vice versa*. The values of permittivity are  $\epsilon = \{2, 4, 6\}$  plotted for the number of layers  $N = 1, 2, 3$ . It has been observed that the polarizabilities of the cylindrical dielectric core  $\alpha_0$ , the first anisotropic shell  $\alpha_1$ , and the second anisotropic shell  $\alpha_2$  can be illustrated as  $\alpha_0 = 1.6364$ ,  $\alpha_1 = 1.6201$ , and  $\alpha_2 = 1.8473$ , respectively, as shown in Fig. 2.

In Fig. 3, we can see that for a variable number of layers, the value of the polarizability when the permittivity of the cover layer  $\epsilon_2 = 4$  has more weight than the case when permittivity of the cover layer is  $\epsilon_2 = 2$ . Similarly, for the case of two layers, the same trend is observed for cover layers with permittivity  $\epsilon_2 = 4$  and  $\epsilon_2 = 2$ . The polarizability of the isotropic multilayer circular cylinder placed in free space by inserting anisotropy ratios  $\gamma_0 = \gamma_1 = \gamma_2 = 1$  is shown in Fig. 3.

In the second part, we describe the cloaking behavior of the PRA multilayer cylinder. For that, we have taken into account Eq. (33), which represents the relationship between the radial and the tangential permittivity components required for invisibility cloaking. Both components have been defined as a function of  $\kappa$ . The permittivity ratio becomes  $\epsilon_t/\epsilon_r = \kappa_k^2$ . For the invisibility cloaking ratio,  $\epsilon_t/\epsilon_r \rightarrow \infty$ . When we have studied simultaneously decreasing radial permittivities and increasing tangential permittivities, both cases can be used for a cloak, as shown in Fig. 4.

Moreover, for the clear vision of cloaking, we have constructed a model of the isotropic layer that is coated with a homogeneous anisotropic multilayer by using COMSOL Multiphysics. We describe the potential distribution of the structure having different parametric values: radius of the inner core  $a = 0.25$  m, first shell

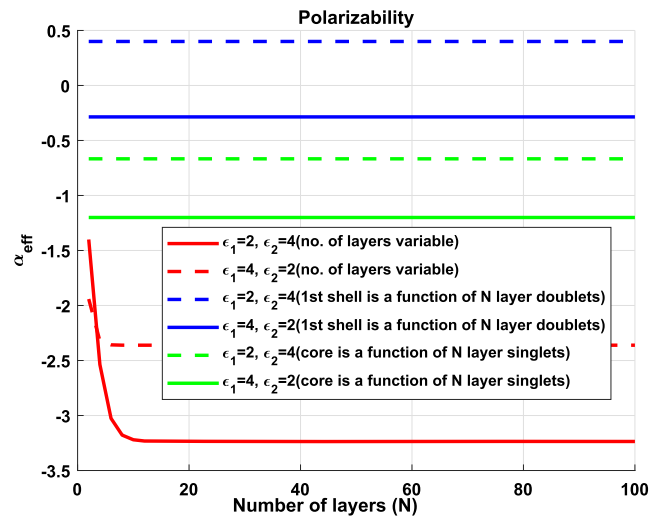


FIG. 3. Normalized polarizability of an isotropic circular cylinder as a function of the number of layers, with the following parameters:  $\epsilon_1 = 2$ ,  $\epsilon_2 = 4$ , and  $\gamma_0 = \gamma_1 = \gamma_2 = 1$ .

$b = 0.5$  m, and second shell  $c = 0.75$  m. Similarly, the radial permittivity of the outer shell is  $\epsilon_{1r} = 8$ , second shell  $\epsilon_{2r} = 4$ , and dielectric core  $\epsilon_{3r} = 1$ ; and the tangential permittivity of the outer core is  $\epsilon_{1t} = 0.125$ , second shell  $\epsilon_{2t} = 0.25$ , and dielectric core  $\epsilon_{3t} = 1$ . This is the preference because relatively moderate anisotropy ratios  $\gamma = \{0.125, 0.25\}$  are required to cloak the core of the cylinder.

Figure 5 presents the potential distribution of the structure in the  $(x-y)$  plane. The homogeneous multi-anisotropic layer makes the potential levels bend toward an approximately constant null

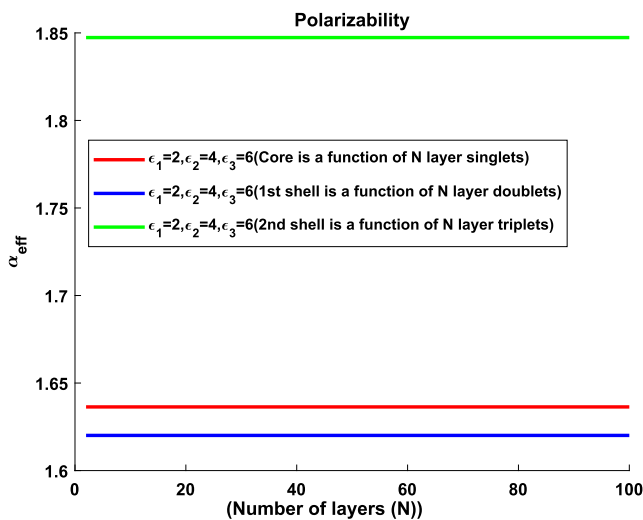


FIG. 2. Normalized polarizability of the PRA circular cylinder as a function of the number of layers, with the following parameters:  $\epsilon_1 = 2$ ,  $\epsilon_2 = 4$ ,  $\epsilon_3 = 6$ ,  $\gamma_1 = 5$ , and  $\gamma_2 = 6$ .

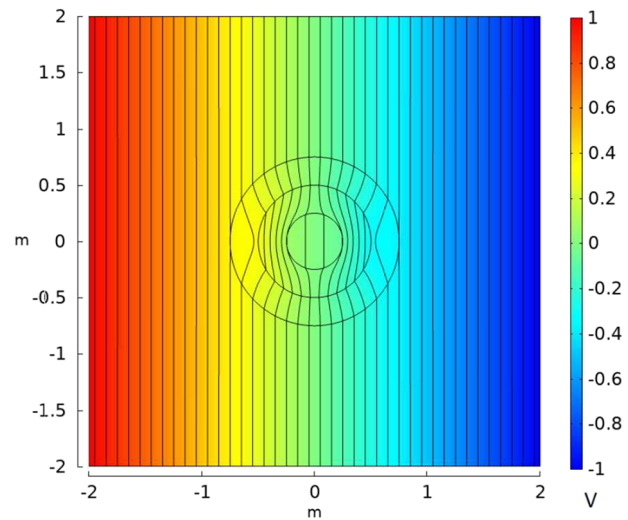
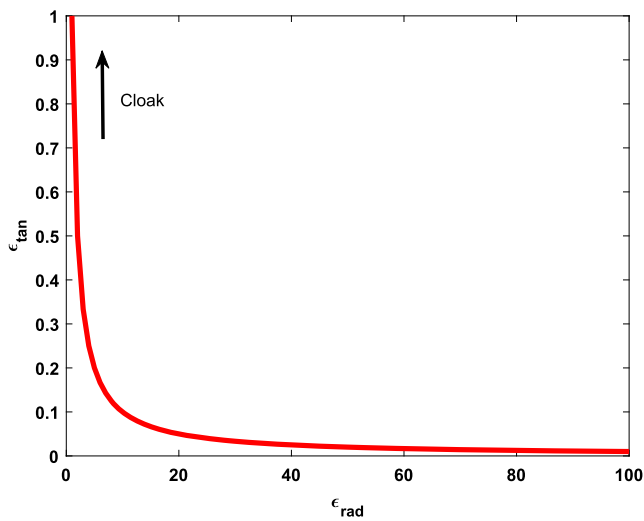


FIG. 4. Potential distribution of a structure, where the anisotropic multilayer circular cylinder with radial permittivities  $\epsilon_r = \{8, 4, 1\}$  and tangential permittivities  $\epsilon_t = \{0.125, 0.25, 1\}$  has been taken.



**FIG. 5.** Anisotropy ratios that make the intact radially anisotropic multilayer cylinder invisible, that is, Eq. (33) plotted on a linear scale.

potential, and a zero-field is produced inside the core, which is required to conceal the inner isotropic layer of the cylinder.

## VI. CONCLUSION

In this article, we have analyzed the behaviors of PRA multilayer circular cylinder geometry in a uniform static field. This model explains cloaking using homogeneous multi-anisotropic layers. It is a more appropriate model rather than the model which is present in the literature with one anisotropic layer surrounding the object, where it is not always possible to retain the same permittivity value everywhere inside the shell. Due to many factors including material loss and absorption, a single layer cannot be homogeneous, which is actually required. Maybe the more elegant way is to discretize a single-layer into homogeneous multilayers. If every layer can be assigned fixed and different permittivity values with an arbitrary number of layers, homogeneity throughout the cloaking model can be achieved. Our cloaking approach is based on a relation between the tangential and the radial variable component of permittivities, which makes the structure more convenient to hide the inner core layer of the cylinder. When the tangential component of permittivity tends to infinity, the radial should approach zero. This trend gives rise to a strong distribution of the electric potential on the surface between the anisotropic multilayer structure and the free space in which it is immersed, whereas the interior cloak surface of the cylinder remains with zero potential. That is how this model satisfies and approaches the invisibility condition. Hence, it is an innovative homogeneous multilayer anisotropic model which can work appropriately for cloaking applications.

## DATA AVAILABILITY

The data that support the findings of this study are available within the article.

## REFERENCES

- J. B. Pendry, D. Schurig, and D. R. Smith, "Controlling electromagnetic fields," *Science* **312**, 1780–1782 (2006).
- D. Schurig, J. B. Pendry, and D. R. Smith, "Calculation of material properties and ray tracing in transformation media," *Opt. Express* **14**, 9794–9804 (2006).
- J. N. Newman, "Cloaking a circular cylinder in water waves," *Eur. J. Mech.: B/Fluids* **47**, 145–150 (2014).
- L. Matekovits and T. S. Bird, "Width-modulated microstrip-line based mantle cloaks for thin single- and multiple cylinders," *IEEE Trans. Antennas Propag.* **62**, 2606–2615 (2014).
- U. Leonhardt and T. G. Philbin, "Transformation optics and the geometry of light," *Prog. Opt.* **53**, 69–152 (2009).
- H. Chen, C. T. Chan, and P. Sheng, "Transformation optics and metamaterials," *Nat. Mater.* **9**, 387–396 (2010).
- M. Hua, Q. Shao-Bo, X. Zhuo, Z. Jie-Qiu, and W. Jia-Fu, "The simplified material parameter equation for elliptical cylinder cloaks," *Chin. Phys. B* **18**, 1850–1867 (2009).
- B. Ivisic, Z. Sipus, and J. Bartolic, "Bandwidth of invisible cloak realized with split ring resonators," in *IEEE Conference on Microwave Techniques (IEEE, 2008)*, Vol. 23, pp. 1–4.
- A. Alú and N. Engheta, "Achieving transparency with plasmonic and metamaterial coatings," *Phys. Rev. E* **72**, 016623 (2005).
- M. G. Silveirinha, A. Alú, and N. Engheta, "Parallel-plate metamaterials for cloaking structures," *Phys. Rev. E* **75**, 036603 (2007).
- S. A. Cummer, B. I. Popa, D. Schurig, D. R. Smith, and J. Pendry, "Full-wave simulations of electromagnetic cloaking structures," *Phys. Rev. E* **74**, 036621 (2006).
- S. Batool, F. Frezza, F. Mangini, and Y. L. Xu, "Scattering from multiple PEC sphere using translation addition theorems for spherical vector wave function," *J. Quant. Spectrosc. Radiat. Transfer* **248**, 1–17 (2020).
- S. Batool, Q. A. Naqvi, and M. A. Fiaz, "Scattering from a cylindrical obstacle deeply buried beneath a planar non-integer dimensional dielectric slab using Kobayashi potential method," *Optik* **153**, 95–108 (2018).
- S. Batool, F. Frezza, F. Mangini, and P. Simeoni, "Introduction of radar scattering application in remote sensing and diagnostics review," *Atmos* **11**, 517–534 (2020).
- L. Gao, T. H. Fung, K. W. Yu, and C. W. Qiu, "Electromagnetic transparency by coated spheres with radial anisotropy," *Phys. Rev. E* **78**, 046609 (2008).
- B. Zhang and B.-I. Wu, "Cylindrical cloaking at oblique incidence with optimized finite multilayer parameters," *Opt. Lett.* **35**, 2681–2693 (2010).
- H. M. Zamel, E. El-Diwany, and H. El-Hennaawy, "Approximate electromagnetic cloaking of a conducting cylinder using homogeneous isotropic multi-layered materials," *J. Electr. Syst. Inf. Technol.* **1**, 82–93 (2014).
- C. W. Qiu, A. Novitsky, H. Ma, and S. Qu, "Electromagnetic interaction of arbitrary radial-dependent anisotropic spheres and improved invisibility for nonlinear-transformation-based cloaks," *Phys. Rev.* **80**, 016604 (2009).
- C. W. Qiu, L. Hu, X. Xu, and Y. Feng, "Spherical cloaking with homogeneous isotropic multilayered structures," *Phys. Rev.* **79**, 047602 (2009).
- S. Batool, M. Nisar, F. Frezza, and F. Mangini, "Cloaking using the anisotropic multilayer sphere," *Photonics* **7**, 52–64 (2020).
- S. Batool, M. Nisar, F. Mangini, and F. Frezza, "Cloaking and magnifying using radial anisotropy in non-integer dimensional space," in *14th European IEEE Conference on Antennas and Propagation (EuCAP) (IEEE, 2020)*, pp. 1–5.
- H. Chen, B.-I. Wu, B. Zhang, and J. A. Kong, "Electromagnetic wave interactions with a metamaterial cloak," *Phys. Rev.* **99**, 149901 (2007).
- H. Kettunen, H. Wallén, and A. Sihvola, "Cloaking and magnifying using radial anisotropy," *J. Appl. Phys.* **114**, 110–122 (2013).
- F. Mangini, N. Tedeschi, F. Frezza, and A. Sihvola, "Homogenization of a multilayer sphere as a radial uniaxial sphere: Features and limits," *J. Electromagnet. Wave* **28**, 916–931 (2014).
- H. Wallén, H. Kettunen, and A. Sihvola, "Singularities or emergent losses in radially uniaxial spheres," in *Proceedings of the International Symposium on Electromagnetic Theory, 2013*.

- <sup>26</sup>C. W. Qiu, L. W. Li, T. S. Yeo, and S. Zouhdi, "Scattering by rotationally symmetric anisotropic spheres: Potential formulation and parametric studies," *Phys. Rev. E* **75**, 026609 (2007).
- <sup>27</sup>A. Sihvola, *Electromagnetic Mixing Formulas and Applications* (The Institution of Electrical Engineers, London, UK, 1999).
- <sup>28</sup>F. Mangini, N. Tedeschi, F. Frezza, and A. Sihvola, "Electromagnetic interaction with two eccentric spheres," *J. Opt. Soc. Am. A* **31**, 783–789 (2014).
- <sup>29</sup>T. Rimpiläinen, Anisotrooppisen pallon sahkoinen vaste, Sec 3.1, 2011.
- <sup>30</sup>A. Sihvola and I. V. Lindell, "Transmission line analogy for calculating the effective permittivity of mixtures with spherical multilayer scatterers," *J. Electromagnet. Wave* **2**, 741–756 (1988).
- <sup>31</sup>F. Frezza and F. Mangini, "Electromagnetic scattering of an inhomogeneous elliptically polarized plane wave by a multilayered sphere," *J. Electromagnet. Wave* **30**, 492–504 (2016).
- <sup>32</sup>Y. Cheng and X. J. Liu, "Three dimensional multilayered acoustic cloak with homogeneous isotropic materials," *Appl. Phys. A* **94**, 25–30 (2009).